EARTHQUAKE ENGINEERING AND STRUCTURAL DYNAMICS, VOL. 26, 967–986 (1997)

DYNAMIC NON-LINEAR ANALYSIS OF REINFORCED CONCRETE SHEAR WALL BY FINITE ELEMENT METHOD WITH EXPLICIT ANALYTICAL PROCEDURE

NORIO INOUE,[1]*† KEJIAN YANG[2]‡ AND AKENORI SHIBATA[3]§

[1]*Department of Architecture, Faculty of Engineering, Tohoku University, Aramaki Aoba-ku, Sendai 980-77, Japan*
[2]*Kozo Keikaku Eng. Inc., 4-38-13, Hon-Cho, Nakano-Ku, Tokyo 164, Japan*
[3]*Disaster Control Research Center, Faculty of Engineering, Tohoku University, Aramaki Aoba-ku Sendai 980-77, Japan*

SUMMARY

A numerical procedure for a dynamic non-linear finite element analysis is proposed here to analyse three-dimensional reinforced concrete shear wall structures subjected to earthquake motions. A shear wall is modelled as a quasi-three dimensional structure which is composed of plane elements considering the in-plane stiffness of orthogonal flange panels. The proposed constitutive model is based on the non-linearity of reinforcement and concrete in which the tension stiffening in tension and the degradation of stiffness and strength in compression of concrete after cracking are considered. The acceleration-pulse method, which is a kind of explicit analytical procedure, is employed to solve the non-linear dynamic equations, where the dynamic equation can be solved without stiffness matrix and so the iterative procedure is not necessary for descending portion of stress–strain relationship caused by cracking and softening after compressive strength in concrete. The damping effect is considered by assuming equivalent viscous damping which can give good cyclic behaviours of inertia force vs. displacement relationships. This analytical method was applied to a test specimen of a reinforced concrete shear wall with a H-shaped section which was vibrated up to failure by using a large-scale shaking table with high -performance in Japan. The test was performed as one of the dynamic model tests for evaluation of seismic behaviour of nuclear reactor buildings. The calculations were performed sequentially from the elastic range to failure. The comparison with the test results shows that this approach has good accuracy. © 1997 by John Wiley & Sons Ltd

Earthquake Engng. Struct. Dyn., **26**, 967–986 (1997)

No. of Figures: 18. No. of Tables: 4. No. of References: 19.

KEY WORDS: dynamic nonlinear analysis; finite element method; quasi-three-dimensional model; explicit analytical procedure; equivalent viscous damping; reinforced concrete shear wall

INTRODUCTION

Reinforced concrete shear walls are so important as earthquake-resistant members of buildings that many experimental and analytical studies have been performed for many years to investigate their non-linear behaviours.

Their static characteristics are studied by experiments for many types of shear walls mostly under cyclic loading to know their hysteretic behaviours. The obtained results are summarized to be applicable to non-linear dynamic response analyses by proposing simplified restoring force characteristics[1] including cracking strength, strength at yielding of reinforcement and ultimate strength. As to analytical aspects the

* Correspondence to: Norio Inoue, Department of Architecture, Faculty of Engineering, Tohoku University, Aramaki Aoba-ku, Sendai 980-77, Japan.
† Associate Professor
‡ Dr. Eng.
§ Professor

CCC 0098–8847/97/090967–20$17·50

Received 2 December 1996
Revised 7 April 1997

non-linear behaviours should be studied as two dimensional problems because of their resisting mechanism and so finite element methods (FEM) are considered to be the most powerful tool. When FEM is adopted, the modelling of the constitutive relationship of reinforced concrete is very important. Collins and Vecchio performed experimental studies of reinforced concrete panels subjected to combined uniform stresses and proposed the compression field theory.[2,3] Based on this theory non-linear FEM analyses were performed for reinforced concrete shear walls[4,5] under monotonically increasing loads to obtain the envelope curve of load vs. displacement relationships and to know their resisting mechanism.[6] Furthermore three-dimensional problems of cylinder and box-shaped shear walls were analysed[7] and cyclic analytical procedures were proposed.[8–10]

But the non-linear behaviours subjected to actual dynamic loads like earthquake motions should be investigated in dynamic conditions. In order to clarify such dynamic behaviours, vibration tests have been performed recently by using shaking tables.[11–13] In these tests the stiffness and ultimate strength of shear walls are so large that a large shaking table is needed to obtain accurate experimental data. This means the necessity of high costs and much labour. As to analytical procedures for dynamic responses in actual design, cantilever models with lumped masses are used in most cases by assuming adequate hysteretic rules and equivalent damping characteristics, which are evaluated from many experimental results. These simple models are effective to know the entire behaviour and considered to be useful for actual design purpose. But they cannot clarify their non-linear behaviour as two-dimensional problems. From this point of view, dynamic analytical procedures by FEM are desired to be developed. Non-linear dynamic response analyses were already performed by a FEM model[14] and a rod element model.[15]

In this study a dynamic non-linear analytical method using FEM in which hysteretic characteristics are modelled for concrete and reinforcement is proposed. This model is a quasi-three-dimensional model considering the in-plane stiffness of orthogonal flange panels to analyse shear walls with box-shaped or H-shaped sections. In the analytical procedure the acceleration-pulse method,[16] which is a kind of explicit integration methods, is adopted to deal with descending portion of stress–strain relationship caused by cracking in tension and softening in compression of concrete.

This proposed method was applied to a reinforced concrete shear wall with a H-shaped section, which was vibrated by a shaking table up to failure. The calculated results are represented comparing with test ones and the applicability of the method is discussed.

FEM MODEL

This FEM analysis is intended to deal with three-dimensional shear walls with box-shaped or H-shaped sections, which are used as main structures in nuclear reactor buildings or shear core structures in ordinary buildings. As these shear walls have flange panels orthogonal to web panels which are the main resisting elements, their total behaviour should be investigated as three-dimensional problems. But when the thickness of each panel is comparatively small compared to the width and height of the panel, it is reasonable to model the structure as a quasi-three-dimensional structure which is composed of plane elements ignoring their out-of-plane bending and shear stiffness. Thus a complex three-dimensional reinforced concrete shear wall-slab structure with non-linearity of the materials is represented by assembling iso-parametric plane elements with four nodes for wall panels and iso-parametric three-dimensional solid elements with eight nodes for a slab on the wall panels. Joint nodes, which tie a wall panel to its orthogonal one and the slab, are defined as three-dimensional nodes in order to model the three-dimensional shear wall structure. An example of a box-shaped shear wall is shown in Figure 1. The wall panel is considered as inelastic material, while the slab is considered as relatively rigid elastic material.

To give a detail expression of the joint nodes in the plane element, Figure 2 shows a simple example of a three-dimensional structure which consists of two pieces of wall panels and idealized by two plane elements including two joint nodes as node 3 and node 4. The total displacement vector $\{U\}$ and the element

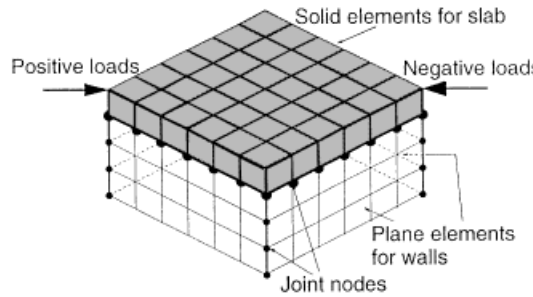

Figure 1. Finite element model of box-shaped shear wall

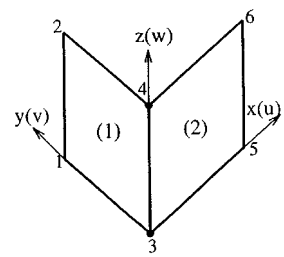

Figure 2. Assumed displacements of each node

displacement vectors $\{U_1\}$ and $\{U_2\}$ can be written as follows.

$$\{U\} = \{v_1 \ w_1 \ v_2 \ w_2 \ u_3 \ v_3 \ w_3 \ u_4 \ v_4 \ w_4 \ u_5 \ w_5 \ u_6 \ w_6\}^{\mathrm{T}} \tag{1}$$

$$\{U_1\} = \{v_1 \ w_1 \ v_2 \ w_2 \ v_3 \ w_3 \ v_4 \ w_4\}^{\mathrm{T}} \tag{2}$$

$$\{U_2\} = \{u_3 \ w_3 \ u_4 \ w_4 \ u_5 \ w_5 \ u_6 \ w_6\}^{\mathrm{T}} \tag{3}$$

The total stiffness matrix related to $\{U\}$ can be obtained by assembling the element stiffness matrices related to $\{U_1\}$ and $\{U_2\}$. In this model only in-plane stiffness is considered for shear wall panels but the compatibility condition of the vertical displacements at joint nodes is satisfied considering a three-dimensional structure. This simplification makes it easier to develop a model which could be applicable to dynamic non-linear analyses of complex three dimensional shear wall structures.

CONSTITUTIVE MODEL OF CONCRETE AND REINFORCEMENT

Constitutive models are formulated on the basis of the non-linearity of concrete and reinforcement which are considered respectively. The smeared approach for both concrete cracks and reinforcements is employed in this model.

Uncracked concrete

The stress-strain relationship in a uni-axial condition is assumed by a multi-linear curve shown in Figure 3, where softening after peak stress in compression is considered. When applying this relationship to the two-dimensional stress field in FEM models, it is assumed that the uncracked concrete is treated as

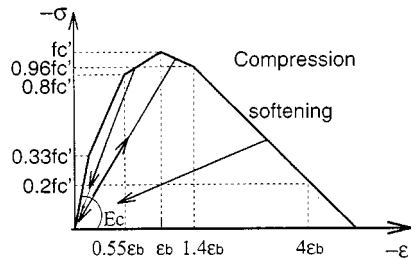

Figure 3. Hysteretic rule of uncracked concrete

a hypothetical isotropic material in an inelastic region.[5] Here the non-linearity is assumed to be determined by the condition of the component in the principal direction i with a larger absolute compressive stress. Thus the material stiffness matrix $[D]_c$ is given by equation (4) in the principal co-ordinates, where the tangential modulus E_i is given by the assumed stress-strain relationship which is obtained for the larger principal stress at uncracked Gauss points of every element. Here v is the Poisson's ratio.

$$[D]_c = \frac{E_i}{1-v^2}\begin{pmatrix} 1 & v & 0 \\ v & 1 & 0 \\ 0 & 0 & \dfrac{1-v}{2} \end{pmatrix} \tag{4}$$

When the structure is under reversing loads, the principal stress–strain relationship is assumed simply returning to the original point linearly. Figure 3 shows the assumed hysteretic rule of uncracked concrete, where fc', ε_b, E_c, are uniaxial compressive strength, strain at maximum compressive stress and Young's modulus, respectively.

Cracked concrete

Cracked concrete is treated as a new material with modified stress–strain characteristics, based on the modified compression field theory proposed by Collins and Vecchio.[2,3] After cracking the material is assumed to be orthotropic with respect to the crack direction and its orthogonal one. Thus the material stiffness matrix of cracked concrete $[D]_c$ is represented by equation (5) in the orthotropic co-ordinates,

$$[D]_c = \begin{pmatrix} E_{c1} & 0 & 0 \\ 0 & E_{c2} & 0 \\ 0 & 0 & G_c \end{pmatrix} \tag{5}$$

where E_{c1} and E_{c2} are the tangential moduli evaluated by the stress–strain relationship of Figure 4 in the compression and tension sides respectively f_{cr} and ε_{cr} are uniaxial tensile strength and strain at maximum tensile stress respectively. G_c is the tangential shear stiffness after cracking. In this study G_c is assumed to be zero considering that the specimen analysed here has cracks with about 45° to the horizontal direction from initial cracking to failure. But if a specimen with rotating cracks is analysed, this factor should be considered precisely. The secondary cracking direction under negative loads is assumed to be orthogonal to the direction of the first crack under positive loads. Here the direction of the local co-ordinate is assumed fixed after initial cracking.

The tension stiffening in tension and the degradation of stiffness and strength in compression are considered after cracking. The degradation ratio of strength in compression should be variable according to tensile strain[3] but in this study it is assumed to be a constant of 0·75 which is considered to be an average

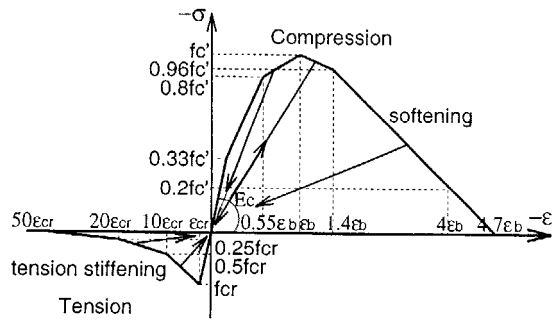

Figure 4. Hysteretic rule of cracked concrete

value in the web panel subjected to shear forces.[17] This value was investigated in the previous analytical study of reinforced concrete shear walls in which the degradation coefficient was variable according to tensile strain.[4]

When the structure is subjected to cyclic loads, the unloading hysteretic rule is assumed to be an origin-oriented model in both tension and compression sides. This type of rule, which has no hysteretic energy consumption for a cyclic loop in a steady state, is commonly used for the shear stress vs. shear strain relationship in a dynamic response analysis of a shear wall using a lumped mass model, where shear deformation is dominant.[1,11,13] Therefore, this simple assumption is reasonable when a shear wall with a small height to depth ratio is analysed. The shortcomings that this rule has no hysteretic energy consumption will be compensated by considering equivalent viscous damping in a dynamic response analysis. The details will be discussed later. Opening or closing of a crack is judged by the sign of strain in the local co-ordinate for cracks considering the origin-oriented hyteretic rule.

Reinforcement

The hysteretic rule of reinforcement is modelled by a bi-linear relationship shown in Figure 5. In order to consider the Bauschinger effect, the reduction of strength is considered when reversing loads are applied. The material stiffness matrix of reinforcement $[D]_s$ is represented by equation (6), where, ρ_x, ρ_y are the reinforcement ratios in the direction x and y respectively, and E_s is the tangential modulus of reinforcement which is determined by the stress–strain relationship shown in Figure 5.

$$[D]_s = \begin{pmatrix} \rho_x E_s & 0 & 0 \\ 0 & \rho_y E_s & 0 \\ 0 & 0 & 0 \end{pmatrix} \tag{6}$$

Constitutive matrix of reinforced concrete

According to the above assumptions, the constitutive matrix of reinforced concrete [D] can be written as equation (7),

$$[D] = [T]_c^T [D]_c [T]_c + [T]_s^T [D]_s [T]_s \tag{7}$$

where $[T]$ is the transformation matrix which is determined by the direction of crack and the direction of reinforcement respectively in every Gauss point of every element. It can be written as equation (8). The angle ψ is given by $\psi = \theta_c + \beta$ for concrete component and $\psi = \theta_s + \beta$ for reinforcement component respectively. Here θ_c and θ_s are the angles of cracking direction and direction of bar arrangement in the local co-ordinate

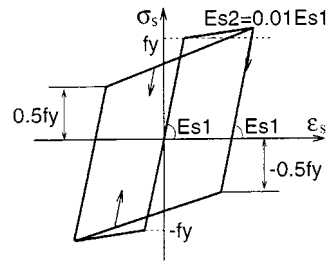

Figure 5. Hysteretic rule of reinforcement

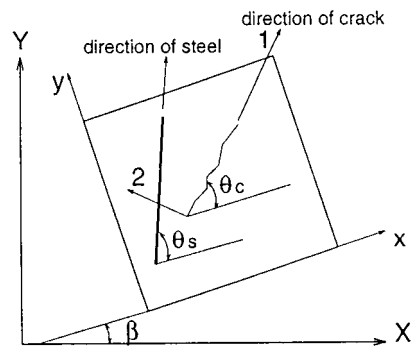

Figure 6. Element in global co-ordinate

respectively and β is the angle of the local co-ordinate to the global one (Figure 6).

$$[T] = \begin{pmatrix} \cos^2\psi & \sin^2\psi & \cos\psi\sin\psi \\ \sin^2\psi & \cos^2\psi & -\cos\psi\sin\psi \\ -2\cos\psi\sin\psi & 2\cos\psi\sin\psi & \cos^2\psi - \sin^2\psi \end{pmatrix} \tag{8}$$

DYNAMIC ANALYTICAL PROCEDURE

To solve the non-linear dynamic equations and obtain the response of structures, it is necessary to choose an efficient numerical method to perform the calculation. Generally speaking, based on the above constitutive models by assuming tangential stiffness and incremental relationships, the average acceleration method is certainly considered as the most suitable tool because it assures unconditional stability.[18] But when applying this approach to the non-linear analysis of reinforced concrete structures with negative tangential stiffness caused by cracking in tension and strain softening in compression after peak stress, some iterative procedure is necessary if unbalance forces are dealt with precisely.

On the other hand the acceleration-pulse method,[16] which is a kind of explicit analytical procedures, is an alternative tool for this kind of problems even though it is not based on incremental relationship and it is conditionally stable. This method is convenient for non-linear analysis of a structure with descending portion of stress–strain relationship because displacements at the next step are calculated from equations of equilibrium at the current step using restoring forces which can be obtained directly by assumed stress-strain relationship. Therefore no iterations need to be performed in non-linear regions with negative tangential stiffness and it can restrain accumulated errors. As to conditional stability it is necessary that time step for

numerical integration should be smaller than a critical value. This disadvantage is overcome by reducing degrees of freedom for the vibration equation.

The damping effect is considered by assuming equivalent viscous damping. It includes viscous damping and hysteretic damping caused by non-linearity of structures. This compensates the defect of the assumption of the origin-oriented hysteretic rule. In actual vibration tests the damping characteristics are usually observed as equivalent damping ratios. Therefore, it is convenient to assume the equivalent viscous damping value referring to the observed results of vibration tests.

Acceleration-pulse method

The dynamic analysis of structures is based on the equations of motion of the system given by equation (9)

$$[M]\{\ddot{X}\} + [C]\{\dot{X}\} + [K]\{X\} = \{F\} \tag{9}$$

in which $[M]$ = mass matrix, $[C]$ = viscous damping matrix, $[K]$ = secant stiffness matrix, $\{\ddot{X}\}$ = acceleration vector, $\{\dot{X}\}$ = velocity vector, $[X]$ = displacement vector, $[F]$ = external force vector for gravity loads and horizontal and vertical seismic loads.

The acceleration-pulse method is based on a direct integration using step-by-step procedures. The basic assumption is to predict the displacements at next step $(n + 1)$ from the displacements at former two steps n and $(n\text{-}1)$, and restoring forces at step n by equations of equilibrium directly. This method is equivalent to the Newmark's β method[18] in which β is zero. Figure 7 shows the basic assumptions of the acceleration-pulse method. Here the acceleration is assumed changing uncontinuously something like an impulse action within a time interval Δt. Because of this, it is referred to as the acceleration-pulse method. The velocity is assumed constant and the displacement is assumed changing linearly within a time interval Δt. According to the above assumptions

$$\{X_{n+1}\} = 2\{X_n\} - \{X_{n-1}\} + \{\ddot{X}_n\}\Delta t^2 \tag{10}$$

$$\{\dot{X}_n\} = (\{X_n\} - \{X_{n-1}\})/\Delta t + 0{\cdot}5\{\ddot{X}_n\}\Delta t \tag{11}$$

where, $\{X_{n+1}\}$, $\{X_n\}$, $\{X_{n-1}\}$ are the displacements at step $(n + 1)$, n and $(n - 1)$ respectively. According to the equation of equilibrium (9)

$$\{\ddot{X}_n\} = -[M]^{-1}[C]\{\dot{X}_n\} - [M]^{-1}\{Q(X_n)\} - \{\ddot{X}_{0n} + \ddot{g}\} \tag{12}$$

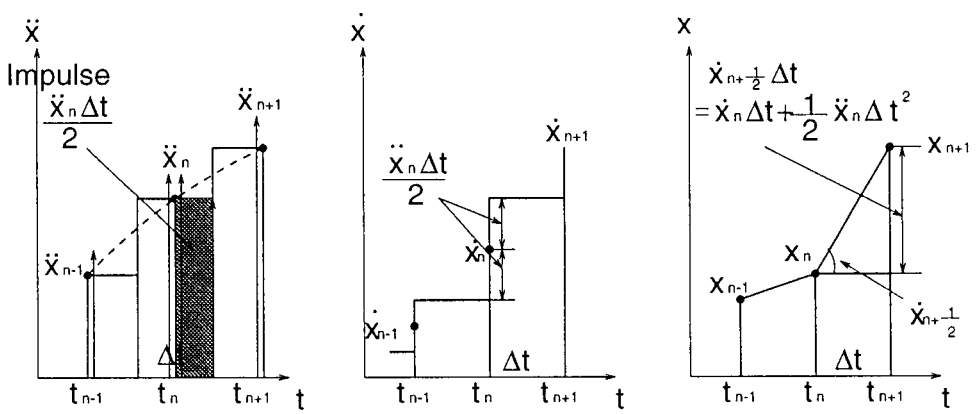

Figure 7. Acceleration-pulse method

where $\{Q(X_n)\}$ is the restoring force vector of a structure which is equal to the $[K]\{X\}$ in equation (9). $\{\ddot{X}_{0n}\}$ is the acceleration vector of ground motions acting as external loads $\{F_n\} = -[M]\{\ddot{X}_{0n}\}$. $\{\ddot{g}\}$ is the acceleration vector of gravity.

Substituting $\{\dot{X}_n\}$ in equation (11) into equation (12) and then substituting $\{\ddot{X}_n\}$ into equation (10) gives

$$\{X_{n+1}\} = ([I] + 0{\cdot}5[M]^{-1}[C]\Delta t)^{-1}(2\{X_n\} - \{X_{n-1}\} + 0{\cdot}5[M]^{-1}[C]\Delta t\{X_{n-1}\} - [M]^{-1}\{Q(X_n)\}\Delta t^2 - \{\ddot{X}_{0n} + \ddot{g}\}\Delta t^2) \tag{13}$$

It should be paid attention to that equation (13) has no stiffness matrix. This formulation gives easy handling of descendibg portion of stress-strain relationship.

Reduction of freedoms

When a reinforced concrete shear wall with a heavy slab like Figure 1 is considered, there is almost no affection if the weight of the web and flange panels is neglected in a dynamic analysis, because they are considerably lighter than those of the slab and additional masses like lead on it. In this study, only the weight of the slab and additional masses is considered as concentrated masses at the nodes of the top slab. Consequently the reduction of freedoms must be done in a dynamic analysis.

Considering reduction of freedoms with respect to the nodes without concentrated masses, the vibration equation (9) is rewritten as

$$\begin{bmatrix} M_1 & 0 \\ 0 & 0 \end{bmatrix} \begin{Bmatrix} \ddot{X}_{n,1} \\ \ddot{X}_{n,2} \end{Bmatrix} + \begin{bmatrix} C_1 & 0 \\ 0 & 0 \end{bmatrix} \begin{Bmatrix} \dot{X}_{n,1} \\ \dot{X}_{n,2} \end{Bmatrix} + \begin{Bmatrix} Q_1(X_n) \\ 0 \end{Bmatrix} = \begin{bmatrix} M_1 & 0 \\ 0 & 0 \end{bmatrix} \{\ddot{X}_{0n}\} - \begin{bmatrix} M_1 & 0 \\ 0 & 0 \end{bmatrix} \{\ddot{g}\} \tag{14}$$

where $[M_1]$ is a mass matrix with respect to the degrees of freedom with concentrated masses. The subscripts 1 in $\{\ddot{X}_{n,1}\}$ and 2 in $\{\ddot{X}_{n,2}\}$ etc. mean the parameters with respect to the degrees of freedom with concentrated masses and without concentrated masses respectively. By the similar deductions, equation (13) is rewritten as

$$\{X_{n+1,1}\} = ([I] + 0{\cdot}5[M_1]^{-1}[C_1]\Delta t)^{-1}(2\{X_{n,1}\} - \{X_{n-1,1}\} + 0{\cdot}5\,[M_1]^{-1}\,[C_1]\Delta t\{X_{n-1,1}\} - [M_1]^{-1}\{Q_1(\mathrm{X}_n)\}\Delta t^2 - \{\ddot{X}_{0n} + \ddot{g}\}\Delta t^2) \tag{15}$$

The velocity and acceleration can be calculated by following equations respectively.

$$\{\dot{X}_{n,1}\} = 0{\cdot}5(\{X_{n+1,1}\} - \{X_{n-1,1}\})/\Delta t \tag{16}$$

$$\{\ddot{X}_{n,1}\} = (\{X_{n+1,1}\} - 2\{X_{n,1}\} + \{X_{n-1,1}\})/\Delta t^2 \tag{17}$$

In order to calculate the displacements with respect to the degrees of freedom without concentrated masses, the total tangential stiffness matrix, $[K(t)]$, which is calculated by the above proposed constitutive model, is used here. It can be rearranged as

$$[K(t)] = \begin{bmatrix} K_{11}(t) & K_{12}(t) \\ K_{21}(t) & K_{22}(t) \end{bmatrix} \tag{18}$$

where the subscripts 1 and 2 in $[K_{ij}(t)]$ are the parameters with respect to the degrees of freedom with concentrated masses and without concentrated masses, respectively.

If the equilibrium condition is written by equation (19) incrementally between steps $(n + 1)$ and n

$$\begin{Bmatrix} \Delta Q_{n+1,1} \\ 0 \end{Bmatrix} = \begin{Bmatrix} K_{11}(t) & K_{12}(t) \\ K_{21}(t) & K_{22}(t) \end{Bmatrix} \begin{Bmatrix} \Delta X_{n+1,1} \\ \Delta X_{n+1,2} \end{Bmatrix} \tag{19}$$

where $\Delta Q_{n+1,1}$ and $\Delta X_{n+1,1}$ are incremental restoring forces and displacements with respect to the degrees of freedom with concentrated masses respectively and $\Delta X_{n+1,2}$ is incremental displacements with respect to the degrees of freedom without concentrated masses. Then the following equation is obtained.

$$\{\Delta X_{n+1,2}\} = -[K_{22}(t)]^{-1}[K_{21}(t)]\{\Delta X_{n+1,1}\} \tag{20}$$

The total displacements with respect to the degrees of freedom without concentrated masses can be calculated by

$$\{X_{n+1,2}\} = \{X_{n,2}\} - [K_{22}(t)]^{-1}[K_{21}(t)]\{\Delta X_{n+1,1}\} \tag{21}$$

where the negative values are used directly in the tangential stiffness matrix after cracking or strain softening of concrete occurs.

As the stiffness matrix is not used in equation (15), the damping matrix $[C_1]$ cannot be defined corresponding to the current stiffness matrix. In this analysis the damping matrix is given by equation (22) assuming that it is proportional to the elastic stiffness matrix, where the proportional coefficient is defined from a degradation ratio of stiffness.

$$[C_1] = \frac{2h_i}{\omega_e}\sqrt{\beta_i}\,[K']_e \tag{22}$$

Here i is the ith vibration step. h_i is the coefficient of equivalent viscous damping. β_i is the corresponding degradation ratio between the secant stiffness at i step, which can be evaluated from a preliminary static non-linear analysis of the structure, and the elastic stiffness of a structure. ω_e is the elastic circular frequency of the structure. $[K']_e$ is the elastic stiffness matrix of the structure which can be calculated by the following equation referring to equations (20) and (21).

$$[K']_e = [K_{11}]_e - [K_{12}]_e[K_{22}]_e^{-1}[K_{21}]_e \tag{23}$$

After the reduction of freedoms, the linear eigen problem equation of a structure for free vibrations can be obtained as

$$[K']_e\{X_1\} = \omega_e^2[M_1]\{X_1\} \tag{24}$$

where $\{X_1\}$ is the displacement vector with respect to the degrees of freedom with concentrated masses.

Algorithm

The algorithm of the acceleration-pulse method for the non-linear dynamic FEM analysis can be summarized as follows.

Step 1: Begin calculation by setting $n = 0$. Calculate the elastic stiffness matrix $[K]$ and the mass matrix $[M]$. Then get the solutions by a static analysis of the structure under gravity loads and the solutions of frequencies and modes of the structure using the equations (23) and (24).

Step 2: Using another numerical method, get the solutions of the displacement, velocity and acceleration at first two steps. The average acceleration method is used in this study.

Step 3: Get strain at every Gauss point from the displacement vector of elements, then calculate the stress vector from strain by proposed constitutive models.

Step 4: The restoring force vector can be obtained from

$$\{Q(X_n)\} = \sum_{\text{element}} \iint [B]^T\{\sigma\}_n \, dV \tag{25}$$

where $[B]$ is the element geometric matrix and $\{\sigma\}_n$ is the element stress vector. Then get the restoring force vector with $\{Q_1(X_n)\}$ respect to the degrees of freedom with concentrated masses.

Step 5: Calculate the damping matrix $[C_1]$ from equations (22) and (23).

Step 6: Calculate the displacement vector $\{X_{n+1,1}\}$ from the displacements at former two steps and other parameters by equation (15).

Step 7: Calculate the velocity vector $\{\dot{X}_{n,1}\}$ and the acceleration vector $\{\ddot{X}_{n,1}\}$ by equations (16) and (17) respectively.

Step 8: Calculate the displacement vector $\{X_{n+1,2}\}$ with respect to the degrees of freedom without concentrated masses by equations (20) and (21). Go to step 3 until the end of a given period of time.

Features of acceleration-pulse method

When adopting the acceleration-pulse method, it must be recognized that the time step Δt for integration should be smaller than a critical value Δt_{cr}, which is calculated in equation (26),[19]

$$\Delta t \leqq \Delta t_{cr} = T_n/\pi \tag{26}$$

where T_n is the smallest natural period of the finite element model with n degrees of freedom. If a time step larger than Δt_{cr} is used, the integration is unstable. This means that some errors resulting from the numerical integration grow and make the response calculations worthless in most cases.

In a dynamic non-linear FEM analysis, if original freedoms were not reduced, the small finite element division might induce that the smallest natural period of the structure would be near zero. An unduly small time step makes it impossible to use the acceleration-pulse method to perform calculations satisfying the condition (26). The reduction procedure given in this study provides an efficient idea to overcome this disadvantage.

NUMERICAL EXAMPLE

The Nuclear Power Engineering Corporation (NUPEC) in Japan has been conducting a project entrusted by the Ministry of International Trade and Industry of Japan entitled 'Elastoplastic Test of Reactor Building'.[12,13] As the main part of this project, 'Model Dynamic Response Test for Evaluation of the Seismic Behavior of Reactor Buildings' was carried out using the large-scale shaking table with high performance at NUPEC's Tadotsu Engineering Laboratory in 1991. The dynamic response behaviours of reinforced concrete shear walls were studied and test data, useful for verification of seismic response analysis codes, were obtained. The details are described in Reference 13. In this study one of the test specimens named U-1 was analysed by the proposed analytical method.

Test specimen

The test specimen was a reinforced concrete shear wall with a H-shaped section shown in Figure 8. The web panel was 75 mm thick, 3000 mm long from centre to centre and 2020 mm in clear height, with a shear span ratio of 0·8. The flange panels were 100 mm thick and 2980 mm long. The reinforcement ratio of the web panel was 1·2 per cent and D6 (deformed bar with a nominal diameter of 6·35 mm) bars with spacing 70 mm were used in double layers. The flange panel was designed longer and thicker than the web one so that stiffness of the orthogonal direction Y was larger than that of the vibrating direction X. But the total volume of reinforcement in the flange panel was equal to the web panel arranging D6 bars sparsely. The calculated design natural frequencies were 13·6 Hz(X) and 14·9 Hz(Y). In order to make the centre of gravity for horizontal direction coincide with the geometrical centre of the top slab of the specimen, additional weights were fixed at the upper and lower surfaces of the top slab, respectively. The total number of the additional lead masses were 24. The total additional weight was 92·9 ton and the total weight including the top slab

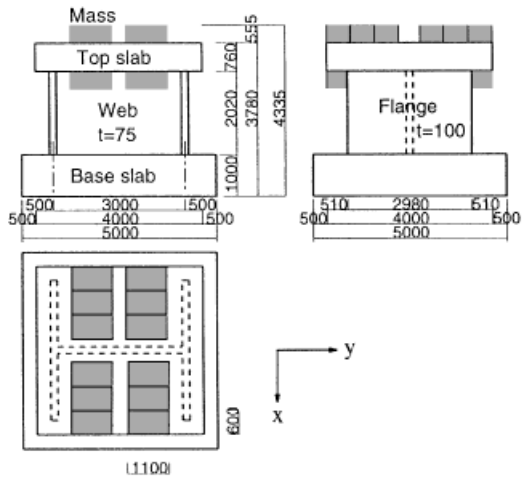

Figure 8. Test specimen

Table I. Material properties of test specimen

Concrete					Reinforceme	
Compressive strength (MPa)	Tensile strength (MPa)	Strain at maximum compressive stress	Young's modulus (MPa)	Poisson's ratio	Yield strength (MPa)	Young's modulus (MPa)
28·6	1·7*	0·0025	$2{\cdot}30\times10^4$	0·155	384	$1{\cdot}84\times10^5$

* $0{\cdot}33\sqrt{f'_c}$

was 122·0 ton. The resulting vertical compressive stress in the wall was 1·47 MPa. Table I summarizes properties of the specimen obtained by material tests. But the tensile strength was calculated by the formula $0{\cdot}33\sqrt{f'_c}$.[3]

Input motion

The objective of this vibration test was to clarify the dynamic response properties of the specimens ranging from elastic to ultimate states. In this test artificial waves were adopted as input motions of the shaking table because they could avoid rapid change in the amplification ratio induced by stiffness changes in the specimen due to plasticity, if the flat part in the spectrum was assumed for the frequency ranging from 14 to 4 Hz corresponding to the initial elastic region to the maximum load, respectively. Figures 9 and 10 show the time history of the input acceleration that was observed at the base slab in RUN-1 and its response spectrum respectively.

In the test, the specimens were only subjected to excitations in the X direction. The vibration test steps were set corresponding to the following series of five target response levels which were sequentially performed as RUN-1 to RUN-5 in Figure 11. For each step, the same artificial wave was input and its amplitude was enlarged gradually. The vibration test program designed can be concluded as follows;

RUN-1: Small-amplitude level in elastic range

RUN-2: Strain level at shear crack initiation, shear deformation angle of about 0·24 /1000 radian

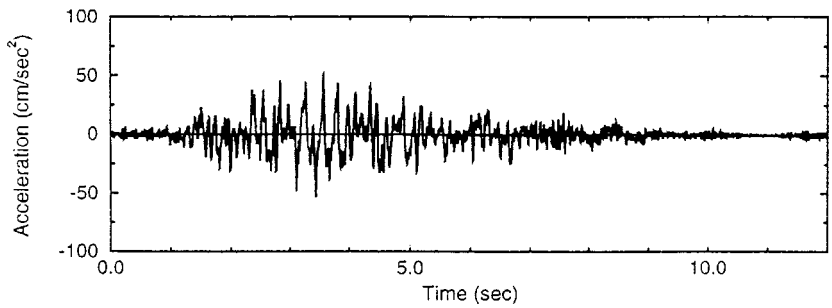

Figure 9. Time history of input acceleration

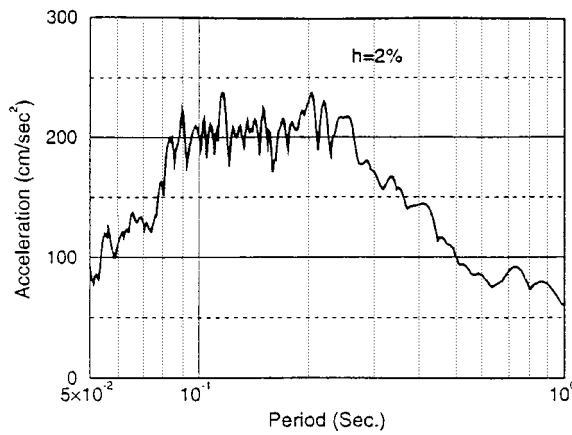

Figure 10. Response spectrum of input acceleration

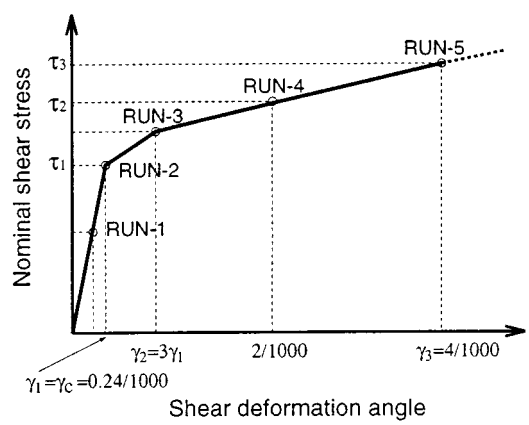

Figure 11. Target response levels of specimen

RUN-3: Strain level at 3 times the above value in RUN-2, shear deformation angle of about 0·72 /1000 radian

RUN-4: Shear deformation angle of about 2 /1000 radian

RUN-5: Vicinity of ultimate strength, shear deformation angle of about 4 /1000 radian

In RUN-2 of the test step for the specimen U-1 which will be analysed in this study, the observed response level was smaller than that of the target response. For this reason, an additional RUN-2′ was carried out actually. So this test had six vibration steps.

Test results

The response maximum values observed are shown in Table II where the input horizontal acceleration of the base slab at the upper surface and the response acceleration, displacement and deformation angle at the top slab are described. The final failure pattern of the specimen is shown in Figure 12. Initial shear cracking at the mid-portion of the web panel and horizontal cracking of the flange panel were observed after RUN-2′ and after RUN-4 respectively. At RUN-5 sliding shear failure occurred at the bottom of the web panel and concrete fell out. Table III shows the change of the natural frequency and the equivalent viscous damping ratio observed. They were determined from the transfer function calculated from the horizontal accelerations of the base slab and the top slab, which were monitored during small amplitude vibration tests performed immediately before each test RUN. The equivalent viscous damping ratio became larger according to the increase of shear strain. These values are very near to observed ones by the shaking table test of a scaled BWR modele.[11]

Analytical model

Because the specimen was only subjected to excitations in the X-direction, the top slab was modelled by plane elements in which a half of the depth of the top slab was chosen as the height of those elements (Figure 13). The stiffness of these elements was increased to represent the solid condition of the top slab.

Table II. Test results

RUN	Input acceleration at base slab (cm/s^2)	Response at top slab		
		Acceleration (cm/s^2)	Displacement (mm)	Deformation angle (1/1000 radian)
RUN-1	58	208	0·30	0·15
RUN-2	122	399	0·61	0·30
RUN-2′	317	602	1·09	0·54
RUN-3	361	738	1·71	0·85
RUN-4	583	895	3·93	1·94
RUN-5	1256	1347	> 20·0 (12·5)*	> 10·0 (6·19)*

* Maximum response displacement and deformation angle at maximum horizontal response acceleration

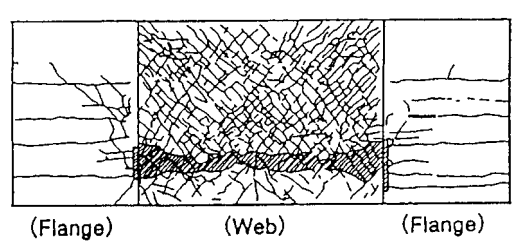

Figure 12. Final appearance after RUN-5

Table III. Change of frequency and equivalent viscous damping ratio

	Frequency (Hz)	Equivalent viscous damping ratio (%)
Before RUN-1	13·2	1·1
Before RUN-3	11·3	2·5
Before RUN-4	9·9	3·0
Before RUN-5	7·7	4·0

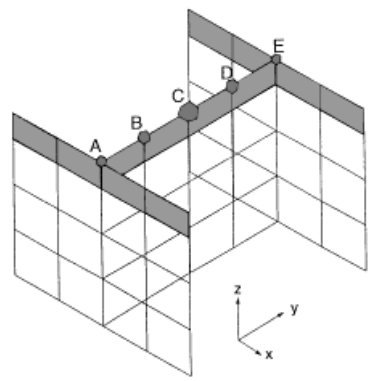

Figure 13. Mesh layout of test specimen

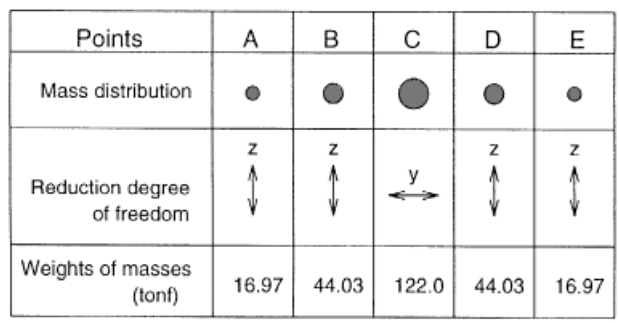

Figure 14. Reduction degrees of freedom and mass distribution

Concentrated masses were arranged on five nodes at the top elements symmetrically according to the total weight 122 ton and the moment of inertia $1{\cdot}259 \times 10^6$ ton cm^2 of the specimen. Reduction degrees of freedom and mass distribution were shown in Figure 14. Here the total weight was placed at the point C so that the horizontal movement was represented by one degree of freedom. The weights were placed separately for vertical movement at the points A, B, D and E to adjust the moment of inertia which induces the rotation movement of the top slab.

The material properties were assumed by the observed results shown in Table I excluding the Young's modulus of concrete which was reduced to equal to the observed initial fundamental period.

As to the input motions of the base slab only horizontal accelerations were considered because the observed vertical accelerations at the base slab were small enough to neglect their influences.

Free vibration modes

Figure 15 shows the calculated free vibration mode shapes, which are represented as the movements of the top slab, and the natural periods. The first mode is a horizontal displacement with rotation of the top slab. This is the main mode which dominates the entire response behaviour of the specimen. The second and the third ones are vertical movement and rotation of the top slab respectively. These three modes are meaningful for the response analysis. The forth and fifth modes are local vertical movements within the top slab and therefore have very few influences when the horizontal response of the top slab is paid attention to. But when the acceleration-pulse method is adopted, these modes have to be covered adopting an adequate time interval Δt which is small enough to fulfill the convergence condition in equation (26). This consideration is very important point to get rational solutions.

Non-linear response analysis

Numerical calculations were performed sequentially from RUN-1 to RUN-5. The input motions were given by the observed horizontal records at the surface of the base slab. The damping matrix was changed according to the increase of deformations but fixed as a constant during each RUN. The degradation ratio of stiffness in equation (22) was assumed by the observed natural periods and the results of a preliminary static FEM analysis for each RUN. The equivalent damping coefficient was decided in accordance with the test results in Table III. Their values are shown in Table IV. The damping coefficient of RUN-i is equal to the value observed before RUN-$(i + 1)$ where the specimen suffered damage by RUN-i. As to RUN-5 this value

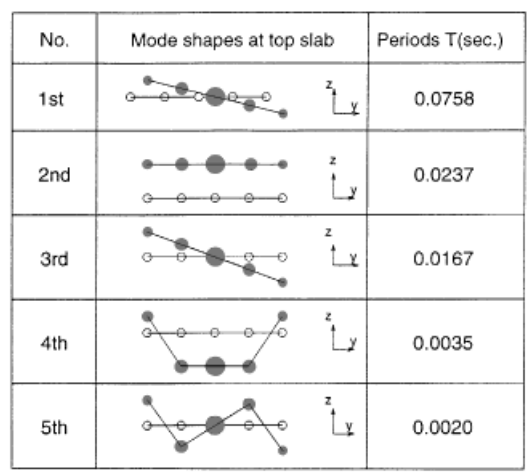

Figure 15. Mode shapes at top slab and natural periods

Table IV. Damping coefficients and corresponding stiffness reduction ratios for analysis

RUN	Damping coefficient (%)	Corresponding stiffness reduction ratio
RUN-1	1·1	1
RUN-2	1·1	0·971
RUN-2′	2·5	0·867
RUN-3	3·0	0·678
RUN-4	4·0	0·357
RUN-5	4·0	0·357

was not obtained because the specimen collapsed. Therefore the value is assumed as the same as RUN-4. The time step of integration Δt was 1/2000 s, which satisfied the convergence condition calculated by equation (26) for the highest mode.

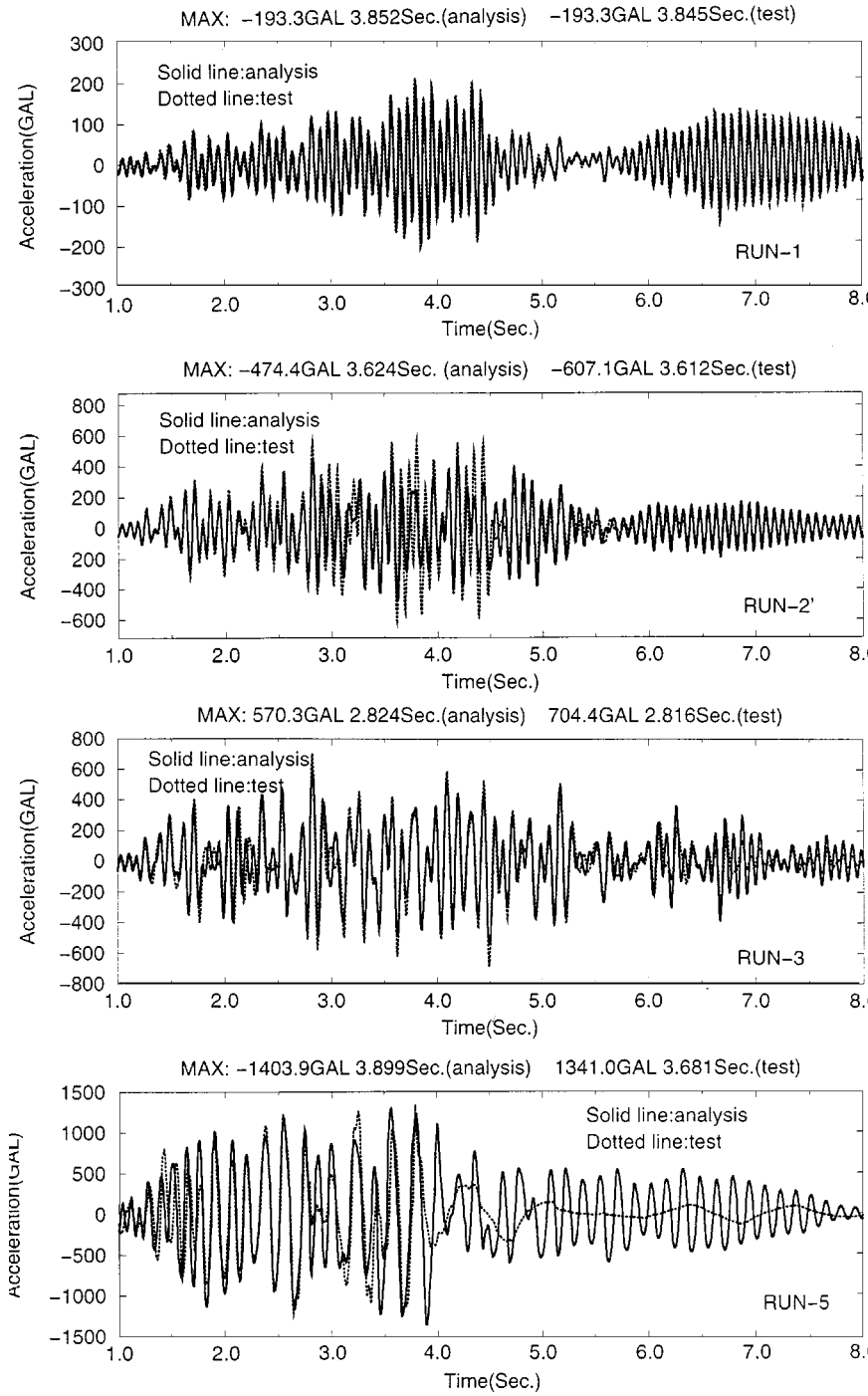

Figure 16. Time histories of acceleration at top slab

The time histories of acceleration are shown in Figure 16 comparing analytical results with test ones. The experimental results are the mean of the observed values at the front and rear sides of the top slab. The observed twisting motion at the top slab was very small in all RUNs. RUN-1 showed an elastic response, where the entire behaviour, the maximum value and the corresponding time were well simulated. These results were obtained for only horizontal input motions ignoring the vertical ones at the base slab but this

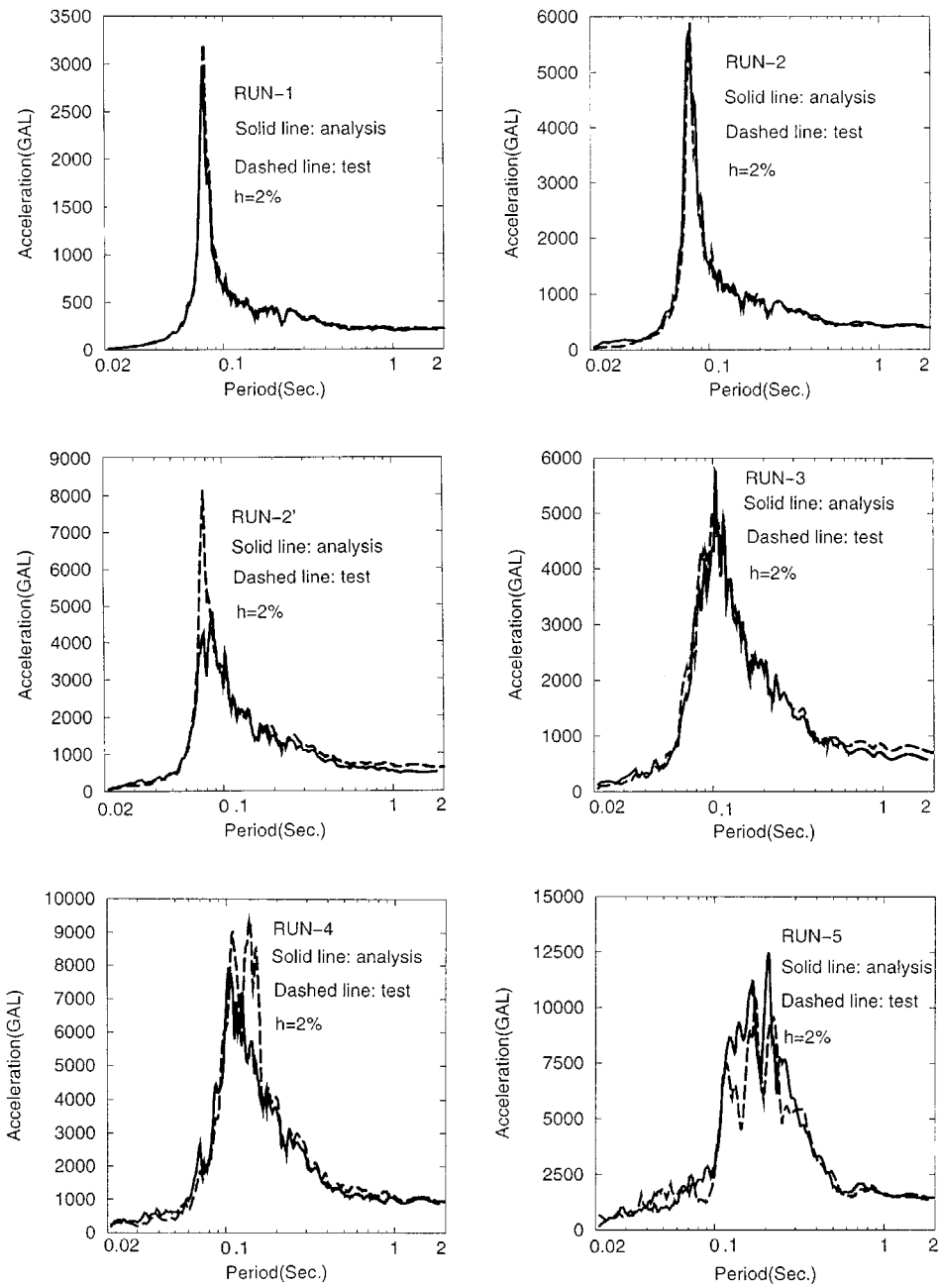

Figure 17. Response spectra of acceleration at top slab

assumption was considered reasonable. In RUN-2′ shear cracks occurred and after that the stiffness decreased rapidly. Because the calculated results estimated a smaller cracking strength which will be well found from Figure 18, the observed behaviour just after cracking was not well represented by this analysis. RUN-3 reached the deformation angle of 0·85/1000 with many cracks. The analytical results showed good

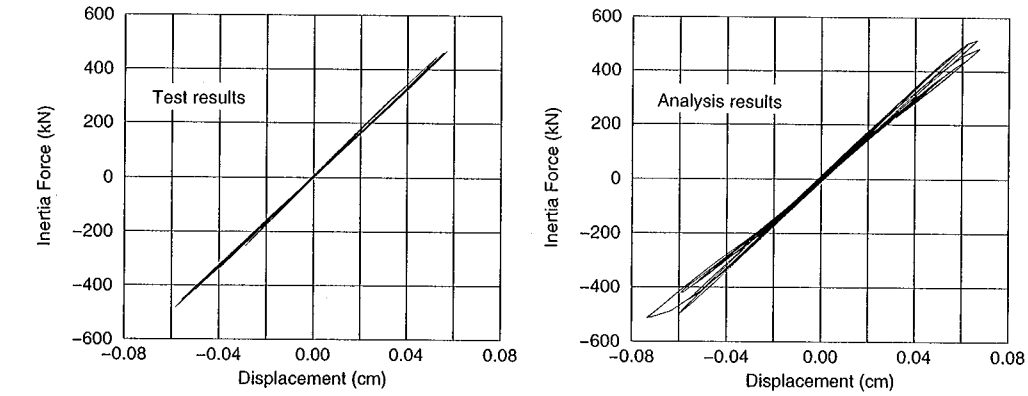

(a) RUN−1 and RUN−2

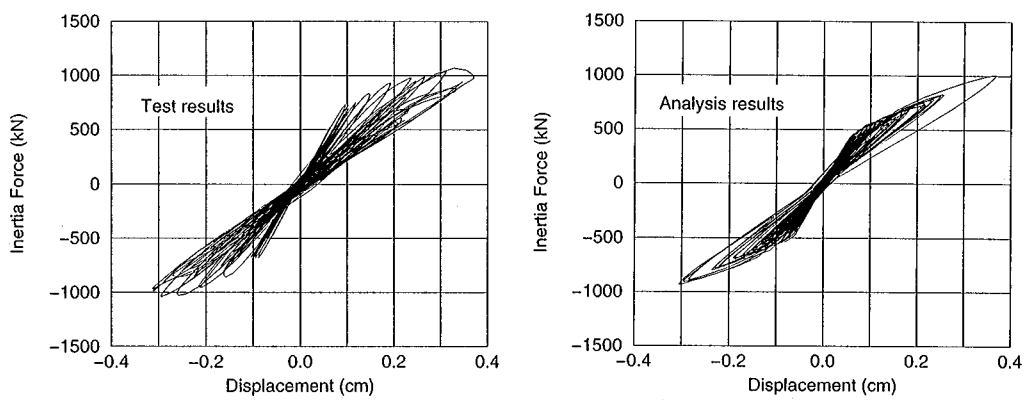

(b) RUN−2′, RUN−3 and RUN−4

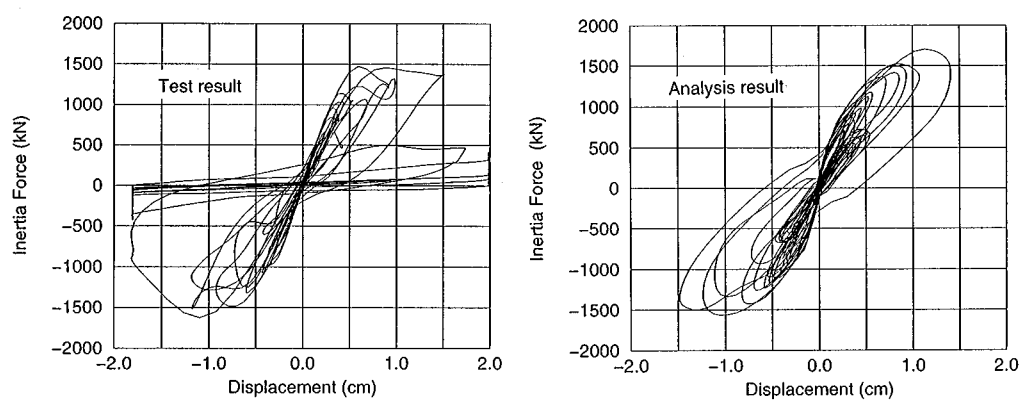

(c) RUN−5

Figure 18. Inertia force vs. displacement relationships

agreement with observed ones during the dominant period. RUN-5 was the final vibration where the shear sliding failure occurred. The observed results were well simulated until the maximum load but after that the behaviour could not be traced.

The time histories of displacement are not presented here but the general tendency is the same as the acceleration. The general behaviour will be understood from the Figure 18 of inertia force vs. displacement relationships.

Figure 17 shows response spectra of acceleration at the top slab in all RUNs. In RUN-1 and RUN-2 the maximum response values were well estimated. In RUN-2′ the stiffness of the test specimen changed rapidly because of shear cracking. This caused the difficulty to estimate well the maximum value by the analysis. RUN-3 showed good analytical results because the specimen behaved comparatively steady condition after many crackings. RUN-4 and RUN-5 were the responses with large deformations where the stiffness changed and several peaks were found in the spectra. The analytical results simulated the tendency that the spectrum had several peaks. The levels of the response values at the peaks were estimated well by this analysis. From the comparative studies of response spectra it can be said that the proposed method predicted the degradation of the specimen according to the increase of input motions.

Figure 18 shows inertia force vs. displacement relationships. Figures 18(a)–18(c) are RUN-1 and RUN-2, RUN-2′ through RUN-4 and RUN-5 respectively. In Figure 18(a) the calculated results estimated the shear cracking strength as a smaller value compared with observed results and the tangential stiffness after cracking was also underestimated. This tendency was shown more clearly in Figure 18(b). It is considered that this result was obtained because the cracking strength calculated by the equation based on static tests might be smaller when applying to dynamic problems and that neglecting shear rigidity after cracking had some influence on the behavior just after shear cracking until steady states with many cracks. But Figure 18(b) shows that the analytical results represented the hysteretic loop which had some surrounded area. In spite of the assumption of the origin-oriented model which neglects hysteretic energy in a steady state, the inertia vs. displacement relationship was well represented by assuming equivalent viscous damping effect adequately. Figure 18 (c) shows RUN-5 which included final failure. The non-linear behaviour before the maximum load was traced but after that it was impossible to follow the test results.

CONCLUSIONS

A dynamic non-linear model by the finite element method is proposed to analyse three-dimensional reinforced concrete shear wall structures subjected to earthquake motions. This model was applied to a reinforced concrete shear wall with a H-shaped section which was vibrated up to failure by a shaking table. The calculated results were compared with the observed test data. The obtained conclusions are as follows.

(1) The analytical results show that this approach had good accuracy for the time histories of acceleration of the top slab, their response spectra and inertia force vs. displacement relationships from the elastic to failure range. This model is effective for dynamic non-linear analyses of three-dimensional reinforced concrete shear wall structures under seismic loading. It is applicable to reactor buildings and other structures which have three-dimensional shear walls with a box-shaped or H-shaped section.
(2) The acceleration-pulse method, which is a kind of explicit analytical procedures, is very effective to non-linear structures which have descending portion of stress–strain relationship caused by cracking in tension and softening in compression. This method has the advantage that no iterations need to be performed in non-linear regions and it can restrain accumulated errors.
(3) When adopting the acceleration-pulse method, it must be recognized that the time step for integration should be smaller than a critical value for the highest mode to get convergence. Sometimes this disadvantage makes its application impossible in actual analyses, but the reduction procedure given in this study provides an efficient idea to overcome it.

(4) The unloading hysteretic rule of concrete was assumed to be an origin -oriented model in both tension and compression sides. This rule gave no hysteretic energy consumption in a cyclic loop of a steady state. But such defect was compensated by considering equivalent viscous damping in a dynamic response analysis, where the observed inertia force vs. displacement relationships were well simulated by the proposed model. But it should be noticed that this hysteretic rule and the equivalent viscous damping coefficients adopted here are applicable to a shear wall structure with a near aspect ratio in which shear deformation is dominant.

ACKNOWLEDGEMENTS

Acknowledgements are due to the Nuclear Power Engineering Corporation (NUPEC) of Japan for performing the vibration test and for providing the test data for this research. Acknowledgements are also due to the Kozo Keikaku Engineering Inc. of Japan for providing the support to complete this analytical work finally.

REFERENCES

1. H. Tanaka *et al*., 'Evaluation method for restoring force characteristics of R/C shear walls of reactor buildings (Parts 1–6)', Summaries of Technical Papers of Annual Meeting, B, AIJ, (1987) 289–230, (in Japanese).
2. M. P. Collins and F. Vecchio, 'The response of reinforced concrete to in-plane shear and normal stresses', ISBN Pub. No. 82-03, University of Toronto, 1982.
3. F. Vecchio and M. P. Collins, 'The modified compression-field theory for reinforced concrete element subjected to shear', ACI, *Struct. J*. **83** (2), 219–231 (1986).
4. N. Inoue, N. Koshika and N. Suzuki, 'Analysis of shear wall based on Collins panel test', FEM Analysis of RC Structure, *Proc. Seminar Sponsored by the Japan Society for the Promotion of Science and U.S. National Science Foundation*, Tokyo, Japan, ASCE, (1985). pp. 288–299.
5. F. Vecchio, 'Nonlinear finite element analysis of concrete membranes', *ACI*, *Struct. J*. **86** (1) 26–35, (1989).
6. N. Inoue and N. Suzuki, 'Microscopic and macroscopic analysis of reinforced concrete framed shear wall', *Proc. Int. Workshop on Concrete Shear in Earthquake held at the University of Houston*, Elsevier Applied Science, Amsterdam, 1991, pp. 333–342.
7. M. Ueda, H. Seya and T. Kei, 'Nonlinear analysis of RC cylinder and box type wall subjected to shear force', *Proc. JCI 2nd Colloq. on Shear Analysis of RC Structures*, 1983, pp.163–172 (in Japanese).
8. D. Darwin and D. A. W. Pecknold, 'Inelastic model for cyclic biaxial loading of reinforced concrete', Structural Res. Ser. No. 409, 1974.
9. H. Okamura and K. Maekawa, *Nonlinear Analysis and Constitutive Models of Reinforced Concrete*, Gihodo, Tokyo, 1991.
10. K. Yang, N. Inoue and A. Shibata, 'Nonlinear FEM analysis of 3-D RC shear walls under cyclic loading', in *Trans. 13th Int. Conf. on Structure Mechanics in Reactor Technology*, Vol. IV, 1995, pp. 249–254.
11. H. Morishita, N. Nakamura, K. Igarashi, N. Inoue and N. Suzuki, 'Simulation analyses on the shaking table test of scaled BWR model', Proc. *10th World Conf. on Earthquake Engineering*, Vol 5, 1992, pp. 2807–2810.
12. T. Nagashima, A. Shibata, N. Inoue and K. Muroi, 'Model tests on dynamic performance of RC shear walls (Dynamic behavior and functional integrity tests on RC shear walls)'; in Trans. *11th Int. Conf. on Struct. Mech. in Reactor Technology*, H, 1991, pp. 259–264.
13. T. Nagashima, A. Shibata, J. Kanda, K. Igarashi, K. Akino and T. Taira, 'Model test and inelastic analysis on dynamic response of RC shear walls', in *Trans. 13th Int. Conf. Struct. Mech. in Reactor Technology*, Vol. III, 1995 pp. 199–204.
14. C. Song and K. Maekawa, 'Dynamic nonlinear finite element analysis of reinforced concrete', J. Faculty Engng. The University of Tokyo (B), **XLI** (1), 73–158, (1991).
15. A. Sakai, T. Maegawa and A. Wada, 'Study on behaviors of reactor building walls subjected to large earthquake', *J. Struct. Construct. Engng. AIJ*, No.447, 97–106 (1993) (in Japanese).
16. C. H. Norris, R. J. Hansen, M. J. Holley Jr., J. M. Bigs, S. Namyet and J. K. Minami, 'Structural Design for Dynamic Loads, McGraw Hill, New York, 1959.
17. I. Shiraishi, Y. Kanoh and N. Machida, 'An analytical study on ultimate shear strength of reinforced concrete shear walls', *J. Struct. Construct. Engng. AIJ*, No.365, 144–155 (1986) (in Japanese).
18. N. M. Newmark, 'A method of computation for structural dynamics', *Proc. ASCE* **85** (EM3), 67–94 (1959)
19. H. Takizawa, 'Study on divergence of numerical integration for vibration equation', *Summaries of Technical Papers of Annual Meeting, AIJ*, 1971, pp. 539–540 (in Japanese).

